blood®
Regular Article

PLATELETS AND THROMBOPOIESIS

The secreted tyrosine kinase VLK is essential for normal platelet activation and thrombus formation

Leila Revollo,[1] Glenn Merrill-Skoloff,[2] Karen De Ceunynck,[2] James R. Dilks,[2] Shihui Guo,[2] Mattia R. Bordoli,[1] Christian G. Peters,[2] Leila Noetzli,[3,4] Andreia Ionescu,[5] Vicki Rosen,[1] Joseph E. Italiano,[3,4] Malcolm Whitman,[1,*] and Robert Flaumenhaft[2,*]

[1]Department of Developmental Biology, Harvard School of Dental Medicine, Boston, MA; [2]Division of Hemostasis and Thrombosis, Department of Medicine, Beth Israel Deaconess Medical Center, Harvard Medical School, Boston, MA; [3]Division of Hematology, Department of Medicine, Brigham and Women's Hospital, Boston, MA; [4]Vascular Biology Program, Boston Children's Hospital and Department of Surgery, Harvard Medical School, Boston, MA; and [5]Department of Biology, Northeastern University, Boston, MA

KEY POINTS

- Platelets lacking secretory pathway tyrosine kinase VLK exhibit defective platelet aggregation, and dense and α-granule release in vitro.
- Mice with platelet-specific deficiency of VLK exhibit decreased thrombus formation after arteriole damage but have normal bleeding times.

Tyrosine phosphorylation of extracellular proteins is observed in cell cultures and in vivo, but little is known about the functional roles of tyrosine phosphorylation of extracellular proteins. Vertebrate lonesome kinase (VLK) is a broadly expressed secretory pathway tyrosine kinase present in platelet α-granules. It is released from platelets upon activation and phosphorylates substrates extracellularly. Its role in platelet function, however, has not been previously studied. In human platelets, we identified phosphorylated tyrosines mapped to luminal or extracellular domains of transmembrane and secreted proteins implicated in the regulation of platelet activation. To determine the role of VLK in extracellular tyrosine phosphorylation and platelet function, we generated mice with a megakaryocyte/platelet-specific deficiency of VLK. Platelets from these mice are normal in abundance and morphology but have significant changes in function both in vitro and in vivo. Resting and thrombin-stimulated VLK-deficient platelets exhibit a significant decrease in several tyrosine phosphobands. Results of functional testing of VLK-deficient platelets show decreased protease-activated receptor 4–mediated and collagen-mediated platelet aggregation but normal responses to adenosine 5′-diphosphate. Dense granule and α-granule release are reduced in these platelets. Furthermore, VLK-deficient platelets exhibit decreased protease-activated receptor 4–mediated Akt (S473) and $Erk_{1/2}$ (T202/Y204) phosphorylation, indicating altered proximal signaling. In vivo, mice lacking VLK in megakaryocytes/platelets display strongly reduced platelet accumulation and fibrin formation after laser-induced injury of cremaster arterioles compared with control mice but with normal bleeding times. These studies show that the secretory pathway tyrosine kinase VLK is critical for stimulus-dependent platelet activation and thrombus formation, providing the first evidence that a secreted protein kinase is required for normal platelet function.

Introduction

Phosphorylation of extracellular proteins has been recognized for more than a century,[1] and a large fraction of proteins secreted into the extracellular space are phosphorylated.[2] Only recently, however, have investigators begun to understand the role that phosphorylation of extracellular proteins serves in modulating protein function outside the cell. An important reason for the gap in knowledge regarding the functional significance of phosphorylation of extracellular proteins was the delay in identifying extracellular kinases. Within the last decade, bioinformatic strategies, coupled with biochemical approaches, have led to the identification of kinases with signal sequences that direct them to the secretory pathway and outside the cell, where they can phosphorylate transmembrane and secreted substrates. Such secretory kinases include serine/threonine kinases such as Fam20C[3] and Drosophila four-jointed,[4] sugar kinases such as Fam20B[5] and SGK196,[6] and the tyrosine kinase VLK/PKDCC, herein referred to as VLK.[7] Of these secretory kinases, only VLK has been confirmed to reside in platelets.

VLK is an ~54-kDa glycoprotein with a 32 amino acid hydrophobic sequence that targets VLK to the secretory pathway and the extracellular environment.[7-9] As a kinase, it exhibits a significant preference for tyrosine; however, no consensus sequence for its phosphorylation has been identified.[7] The catalytic activity of VLK seems to be necessary for its own secretion, as kinase-dead mutants are not secreted. It has diverse cellular functions such as mediating axonal branching by phosphorylating repulsive guidance molecule b,[9] regulating Hedgehog signaling,[10] modifying phosphorylation of extracellular matrix proteins in the

trabecular meshwork of the eye,[11] and phosphorylating several components of the endoplasmic reticulum–proteostasis machinery.[12] Targeted disruption of the gene that encodes VLK (ie, *Pkdcc*) in mice results in perinatal death and impaired skeletal, intestinal, and lung development.[8,13] Genome-wide association studies associate VLK with increased fracture risk in humans[14] and flight efficiency in birds.[15] Biallelic gene-disrupting variants in VLK have been identified in 2 individuals with marked skeletal abnormalities.[16] Regulated secretion of endogenous VLK was first established in platelets,[7] and evaluation of the platelet phosphotyrosine proteome reveals phosphorylation of several secreted proteins and extracellular domains of membrane proteins (supplemental Table 1, available on the *Blood* Web site)[17-20]; however, the effect of VLK deficiency on platelet function has not previously been evaluated.

To understand the contribution of tyrosine phosphorylation of secreted factors and extracellular domains of transmembrane proteins in platelet function, we examined the effects of loss of VLK in platelets. Mice with a megakaryocyte/platelet-specific deficiency of VLK were generated and their platelets evaluated. Platelets from these mice were normal in number and morphology but defective in phosphorylation of tyrosine and stimulation-dependent aggregation. Mice lacking platelet VLK displayed normal bleeding times but with a substantial defect in thrombus formation after laser-induced damage of cremaster arterioles. These results show a novel role for the secretory pathway tyrosine kinase VLK in platelet function and thrombus formation, and they provide the most compelling evidence to date that secreted kinases contribute to platelet function.

Materials and methods

Liquid chromatography/tandem mass spectrometry

Human platelets were isolated from blood collected from 12 healthy donors as described in the supplemental Methods and in accordance with the Beth Israel Deaconess Medical Center Institutional Review Board and the principles of the Declaration of Helsinki. Cell pellets were solubilized with radioimmunoprecipitation assay (RIPA) buffer followed by acetone (MilliporeSigma) precipitation. Lysates were processed as previously described for phosphotyrosine site identification at the Mass Spectrometry Core in the Beth Israel Deaconess Medical Center.[21] Tryptic digests were injected to an Orbitrap Elite mass spectrometer (Thermo Fisher Scientific) using EASY-NLC II nanoflow high-performance liquid chromatography. Raw tandem mass spectrometry fragmentation data were analyzed with Andromeda integrated to MaxQuant software with a false discovery rate of 1% vs the human protein database.

Cell culture, transfection, and cloning

293T cells (ATCC) were grown in Dulbecco's modified Eagle's medium supplemented with 10% (vol/vol) fetal bovine serum and 1X penicillin/streptomycin/amphotericin B (Lonza) at 37°C with 5% carbon dioxide. Cells were transfected with Lipofectamine 2000 (Thermo Fisher Scientific) according to the manufacturer's protocol. All VLK plasmids and synovial K4 cell lines have been previously described.[7] Human and mouse ENTPD6 cDNA (Sino Biological) lacking the stop codon was subcloned into plasmid modified from the pCS2^{+} expression vector containing a C-terminal V5 tag to generate plasmids expressing human or mouse ENTPD6-V5.

Protein isolation, purification, and immunoblotting

Cells were lysed in RIPA buffer with protease and phosphatase inhibitors. For RIPA-resistant extracts, remaining pellets after RIPA extraction were washed and reconstituted in 1% sodium dodecyl sulfate (SDS). Lysates were immunoprecipitated with anti-V5 beads (MilliporeSigma) and eluted with epitope-specific peptide (Tufts University Core). Phosphotyrosine immunoprecipitations were conducted with anti-phosphotyrosine (anti–p-Tyr) agarose-coupled beads clone 4G10 (MilliporeSigma) and Sepharose-coupled beads P-Tyr-1000 (Cell Signaling Technology). Phenyl phosphate (MilliporeSigma) was used to control nonspecific binding to beads. VLK was immunoprecipitated with antibody raised against the GELKVTDLDDARVEETPC epitope of VLK (AbFrontier) conjugated to protein A agarose and eluted with epitope-specific peptide (Tufts University Core). Thrombospondin 1 (Tsp1) was immunoprecipitated with anti–Tsp1 antibody (Cell Signaling Technology, #D7E5F) conjugated to protein A agarose and eluted with 2% SDS. Samples were examined by immunoblotting after SDS–polyacrylamide gel electrophoresis with 8%, 16%, or 4% to 12% gradient gels (Thermo Fisher Scientific). The following primary antibodies were used for protein immunoblots: anti–p-Tyr (4G10, MilliporeSigma, #05-321; P-Tyr-1000, Cell Signaling Technology, #8954), anti–V5-horseradish peroxidase (Thermo Fisher Scientific, #46-0708), anti-ENTPD6 (GeneTex, #GTX101851), anti-VLK raised against epitopes SRAEYQRIPDSAITQEDYR of mouse and RQLVFFKTGWSQVVPDPNKTTYVKASG of human VLK (AbFrontier), anti–p-VLK (Y64) raised against epitope GRGELARQIRERYEEVQRYSRG phosphorylated at Y64 of mouse VLK (AbFrontier), anti-cytoplasmic actin (MilliporeSigma, #A4700), anti–glyceraldehyde-3-phosphate dehydrogenase (GAPDH)–horseradish peroxidase (GeneTex, #GTX627408-01), anti–p-Akt (S473) (Cell Signaling Technology, #4060), anti-Akt (Cell Signaling Technology, #4691), anti–p-Erk$_{1/2}$ (T202/Y204) (Cell Signaling Technology, #4370), anti-Erk$_{1/2}$ (Cell Signaling Technology, #4695), anti–P-selectin (R&D Systems, #AF737), anti–integrin β3 (Cell Signaling Technology, #13166), anti–integrin α2b (Boster, #PB9647), anti–fibrinogen-γ (GeneTex, #GTX108640), anti-von Willebrand factor (vWR) (Dako, #A0082; Santa Cruz Biotechnology, #sc-271409), anti–platelet factor 4 (PF4) (R&D Systems, #AF595), anti–glycoprotein Ibα (Emfret Analytics, #M043-0), and anti-Tsp1 (Bethyl, #A304-989A-M). Image acquisition was performed with a PXi4 Chemiluminescent and Fluorescent Imaging System (Syngene). Quantification of percent protein phosphorylation and total protein levels were performed with Adobe Photoshop 2020.

Transgenic mice

Vlk$^{flox;neo}$ mice[22] were a generous gift from Aimée Zuniga. Introduction of a neo cassette in the reverse orientation in the Vlk locus of *Vlk*$^{flox;neo}$ mice renders the *Vlk* allele hypomorphic, resulting in perinatal lethal homozygous mice. To remove the neo cassette, *Vlk*$^{flox;neo}$ mice were crossed with FLP1 mice (JAX stock #003946). FLP1-mediated recombination resulted in deletion of the NEO cassette flanked by *frt*- sequences in the resulting offspring (*FLP1; Vlk*$^{flox;neo}$ mice), which were then mated with wild-type mice to remove the FLP1 transgene. The resulting

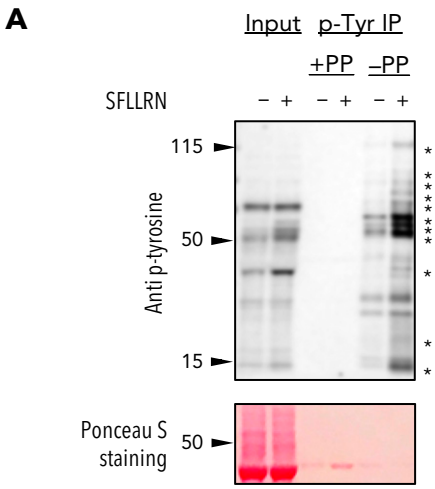

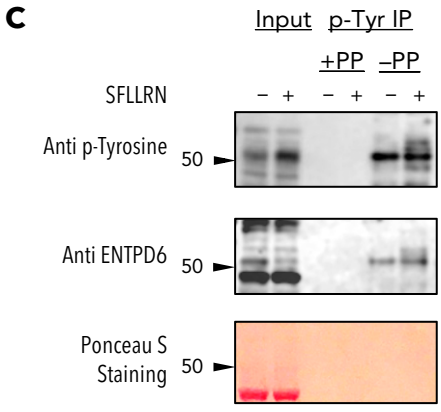

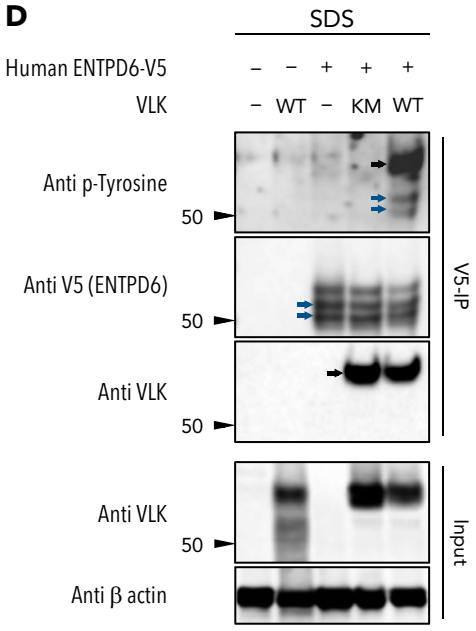

B

Protein Name (Gene name)	Phospho-site	Intensity rank	Information phosphosite
Ectonucleoside triphosphate diphosphohydrolase 6 (ENTPD6)	Y290	21	Tyrosine conserved among ENTPD family members
Platelet basic protein (PPBP)	Y58	42	Tyrosine near cleavage site to generate Neutrophil-Activating Peptide 2
Integrin alpha-IIb (ITGA2B)	Y402	107	Tyrosine within calcium binding domain
Multimerin-1 (MMRN1)	Y330	211	–

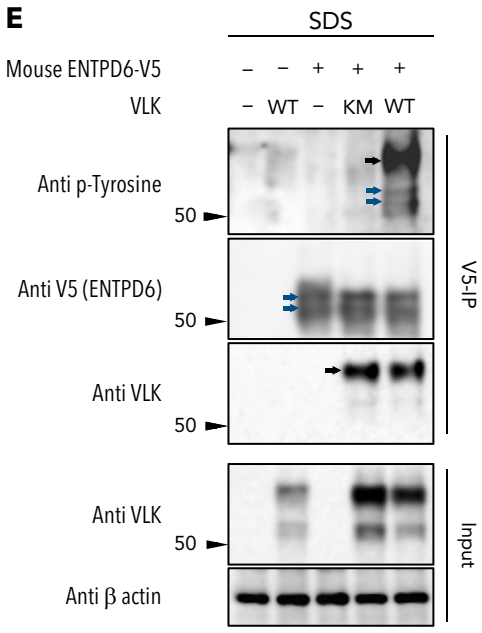

Figure 1. Evaluation of extracellular tyrosine phosphorylation of proteins in human platelets. (A) p-Tyr protein levels in total (Input) and p-Tyr immunoprecipitated fraction (p-Tyr IP) from platelet lysates were assessed by using western blot analysis. Phenyl phosphate (PP) was used as negative control for nonspecific binding to p-Tyr beads, and Ponceau S staining was used to examine total protein levels in input samples. Asterisks indicate activation-dependent tyrosine phosphorylation. (B) Phosphorylated tyrosine peptides isolated by anti–p-Tyr IP of tryptic digests from thrombin receptor activating peptide (TRAP)-stimulated human platelet lysates were analyzed by using liquid chromatography/tandem mass spectrometry. A total of 213 unique phosphopeptides were identified; within this pool, 4 tyrosine phosphosites were mapped to proteins with

heterozygous progeny ($Vlk^{flox/+}$) were subsequently mated to obtain homozygous $Vlk^{flox/flox}$ mice, herein referred to as $Vlk^{f/f}$. $Vlk^{f/f}$ mice are viable, morphologically normal, born with correct Mendelian frequency, and fertile. To conditionally ablate *Vlk* in cells of the megakaryocytic lineage, $Vlk^{f/f}$ female mice were bred to male mice expressing *Cre* under the control of the platelet factor 4 (Pf4) promoter (*Pf4-Cre*)[23] resulting in $Vlk^{f/f}$; *Pf4-Cre* mice (*Vlk-cKO*). For genotyping, polymerase chain reaction (PCR) was performed on genomic DNA isolated from mouse tails by using the HotSHOT method.[24] Primers to detect Vlk^{fl} allele were: 5.4 F, 5′-cacacgctcaatcataccacacc-3′ and 3.7 R, 5′-ggtcattaggtcacagggtaggg-3′. They yield 2 PCR products at 350 bp and 241 bp corresponding to the flox or wild-type allele, respectively. Primers to detect *Pf4-Cre* allele were: F, 5′-cccatacagcacacctttg-3′ and R, 5′-tgcacagtcagcaggtt-3′.[23] They yield a single PCR product at 450 bp corresponding to *Pf4-Cre* amplicon.

All experiments were performed with 10- to 14-week-old male mice, and littermate $Vlk^{f/f}$ mice were used as controls. Mice were housed in a room maintained at 25°C, on a 12-hour light/dark cycle, and fed regular chow ad libitum. All procedures involving mice were conducted under the approval of the Harvard Medical Area Institutional Animal Care and Use Committee.

Intravital microscopy of laser-induced arteriolar thrombosis

Intravital microscopy of microcirculation in the cremaster arteriole was done using laser injury as previously described.[25] Mice were anesthetized with pentobarbital (5 mg/kg) administered via jugular vein cannula to maintain anesthesia throughout the procedure. Fibrin generation and platelet accumulation were detected at the injury site with DyLight 488–labeled anti-fibrin antibody (59D8, 0.5 μg/g body weight) and DyLight 649–labeled anti-CD42b antibody (M040-3, 0.1 μg/g body weight) injected through a jugular vein catheter. Median fluorescence values over time in >30 thrombi in 3 to 4 mice per genotype were analyzed by using SlideBook 6.0 (Intelligent Imaging Innovations).[26-28] Area under the curve was calculated for individual thrombi and compared between $Vlk^{f/f}$ and *Vlk-cKO* mice to evaluate statistical significance.

Tail bleed assay

Tail bleeding assay was performed as previously described.[29] Briefly, tails from 6 to 7 mice per genotype were surgically dissected 3 mm from the tip, immersed in buffered saline prewarmed at 37°C, and time to bleeding cessation was recorded within 20 minutes.

Methods for electron microscopy, platelet isolation, platelet aggregation, dense granule secretion assay, P-selectin surface expression assay, and statistical analysis are provided in the supplemental Methods.

Results

Tyrosine phosphorylation of luminal or extracellular domains of transmembrane and secreted proteins in platelets

To study phosphorylation on tyrosine residues in extracellular domains of transmembrane and secreted proteins in platelets, we first detected proteins that are tyrosine phosphorylated in platelet lysates in an activation-dependent manner, and subsequently used an informatics-based approach to identify specific proteins and their respective phosphosites. Platelets were stimulated by using SFLLRN, and phosphoproteins were then immunoprecipitated by using an anti–p-Tyr antibody. Immunoprecipitation performed in the presence of phenyl phosphate, a competitive inhibitor of anti–p-Tyr binding,[30] was used to assess nonspecific binding to beads, which was negligible (Figure 1A). Proteins that became phosphorylated in response to PAR1 activation were identified by using mass spectroscopy. This analysis identified 213 unique phosphopeptides (supplemental Table 2). Within this pool, 4 tyrosine phosphosites were mapped to proteins with signal peptides or extracellular domains on transmembrane proteins as annotated in UniprotKB (Figure 1B). Among the tyrosine phosphoproteins identified, we focused our attention on ectonucleoside triphosphate diphosphohydrolase 6 (ENTPD6/CD39L2), a member of the CD39/NTPDase family of ectonucleotidases known to regulate platelet activation and thrombus formation.[31,32] Our study revealed Y290, a residue conserved among NTPDase family members, as a site phosphorylated in ENTPD6 in activated platelets (Figure 1B; supplemental Table 2). Evaluation of platelet lysates showed that a band corresponding to the molecular weight of ENTPD6 is phosphorylated at tyrosine (Figure 1C). Anti–p-Tyr immunoprecipitates from both resting and stimulated platelets identify ENTPD6, confirming that it is tyrosine phosphorylated.

Because VLK is a secretory tyrosine kinase found in platelet α-granules,[7] we evaluated whether cotransfection of 293T cells with VLK and ENTPD6-V5 increased phosphorylation of the enzyme. Analysis of V5 immunoprecipitates from detergent-extracted cells showed increased phosphotyrosine in the presence of wild-type VLK but not in the presence of a kinase-dead mutant VLK for both human (Figure 1D) and mouse (Figure 1E) ENTPD6-V5. These findings confirm that ENTPD6 can serve as a substrate for VLK, consistent with the possibility that VLK is responsible for the observed tyrosine phosphorylation of endogenous ENTPD6. Phosphorylation of ENTPD6 does not change substantially with platelet activation, suggesting that it is phosphorylated in the secretory pathway at some point before platelet activation.

Megakaryocyte/platelet-specific deletion of VLK in mice

VLK-deficient mice die within 1 day after birth.[9,13] To evaluate the function of platelets that lack VLK, we crossed VLK floxed mice ($Vlk^{f/f}$) with mice expressing the Cre recombinase under the control of the PF4 promoter (PF4-Cre mice), resulting in

Figure 1 (continued) signal peptides or extracellular domains on transmembrane proteins as annotated in UniprotKB. (C) ENTPD6 (CD39L2) levels were determined in total (Input) and p-Tyr IP fraction in lysates from human platelets. Total protein levels in input were determined with Ponceau S staining. Tyrosine phosphorylation of V5 immunoprecipitates in RIPA-resistant extracts (SDS) from 293T cells coexpressing V5-tagged human (D) or mouse (E) ENTPD6 with wild-type (WT) or kinase-dead (KM) VLK. Extracts (Input) were analyzed for VLK and actin. Blue and black arrows indicate bands corresponding to ENTPD6 and VLK, respectively.

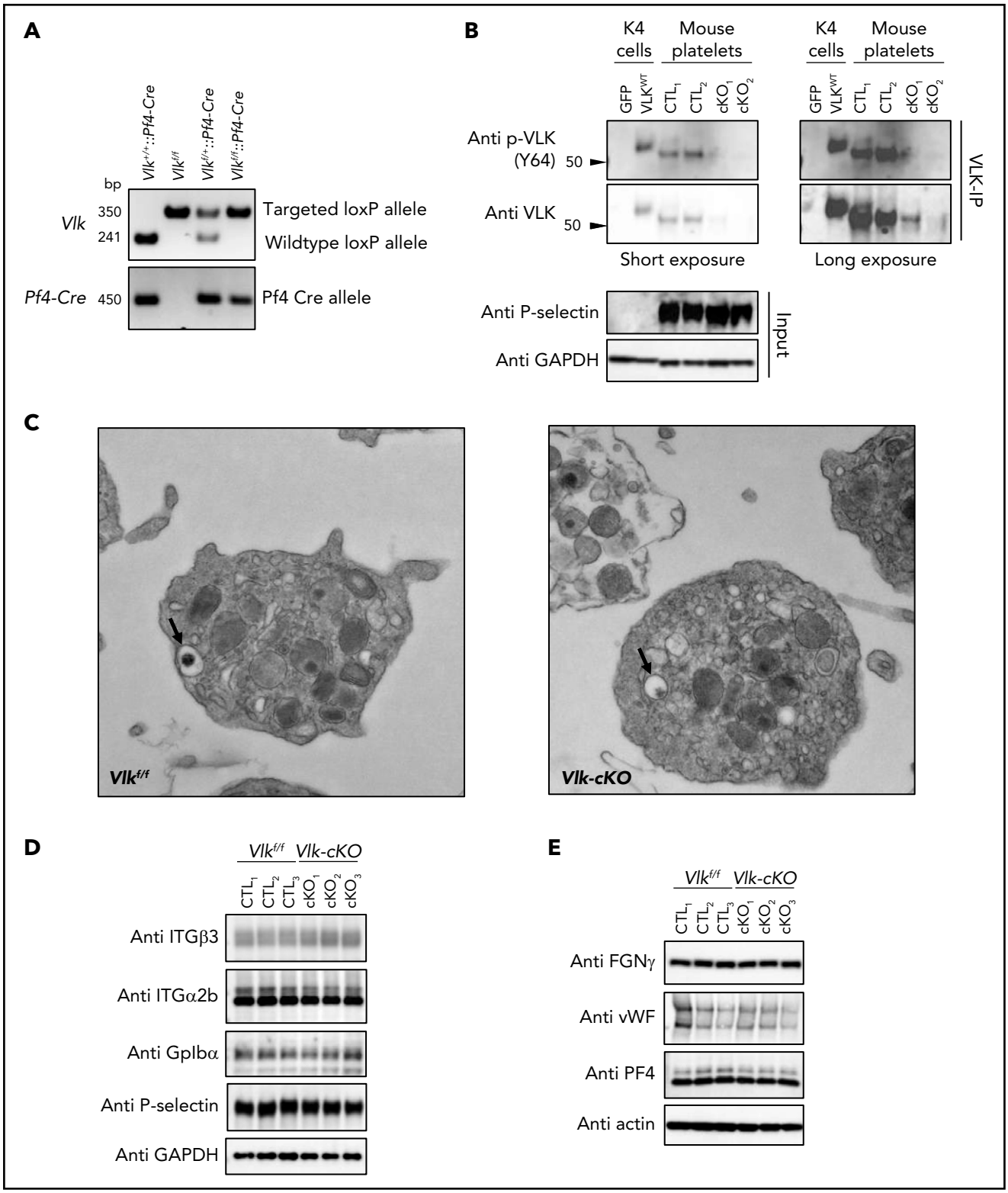

Figure 2. *Vlk* deficiency in platelets does not affect platelet morphology or levels of platelet receptors and cargo proteins. (A) Analysis of genomic DNA from *Vlk*$^{+/+}$::*Pf4-Cre*, *Vlk*$^{f/f}$, *Vlk*$^{f/+}$::*Pf4-Cre*, and *Vlk*$^{f/f}$::*Pf4-Cre* mice. Targeted *loxP* allele (*fl*) is 350 bp; *wildtype* allele (+) is 241 bp; and *Pf4-Cre* allele is 450 bp. (B) Western blot analysis of phosphorylated and total VLK immunoprecipitates (VLK-IP) prepared from *Vlk*$^{f/f}$ (CTL) and *Vlk-cKO* (cKO) washed platelet lysates. Lysates from K4 synoviocytes stably expressing green fluorescent protein (GFP) or wild-type mouse VLK (VLK^{WT}) were used as controls for VLK protein. Eluates were treated with PNGase-F. Anti–P-selectin and GAPDH were used as controls for platelet-specific and total protein levels in input samples, respectively. (C) Representative image of electron microscopy analysis of resting *Vlk*$^{f/f}$ and *Vlk-cKO* platelets. Dense granules are indicated by black arrows. Representative images were obtained at 13000×. Protein levels in platelets from *Vlk*$^{f/f}$ (CTL) and *Vlk-cKO* (cKO) mice (n = 3 mice per genotype). Anti-GAPDH and actin antibodies were used to examine total protein levels of platelet receptors integrin (ITG) β_3, integrin α_{2b}, glycoprotein Ibα (GpIbα), and P-selectin (D) as well as platelet cargo fibrinogen (FGN), von Willebrand factor (vWF), and PF4 (E).

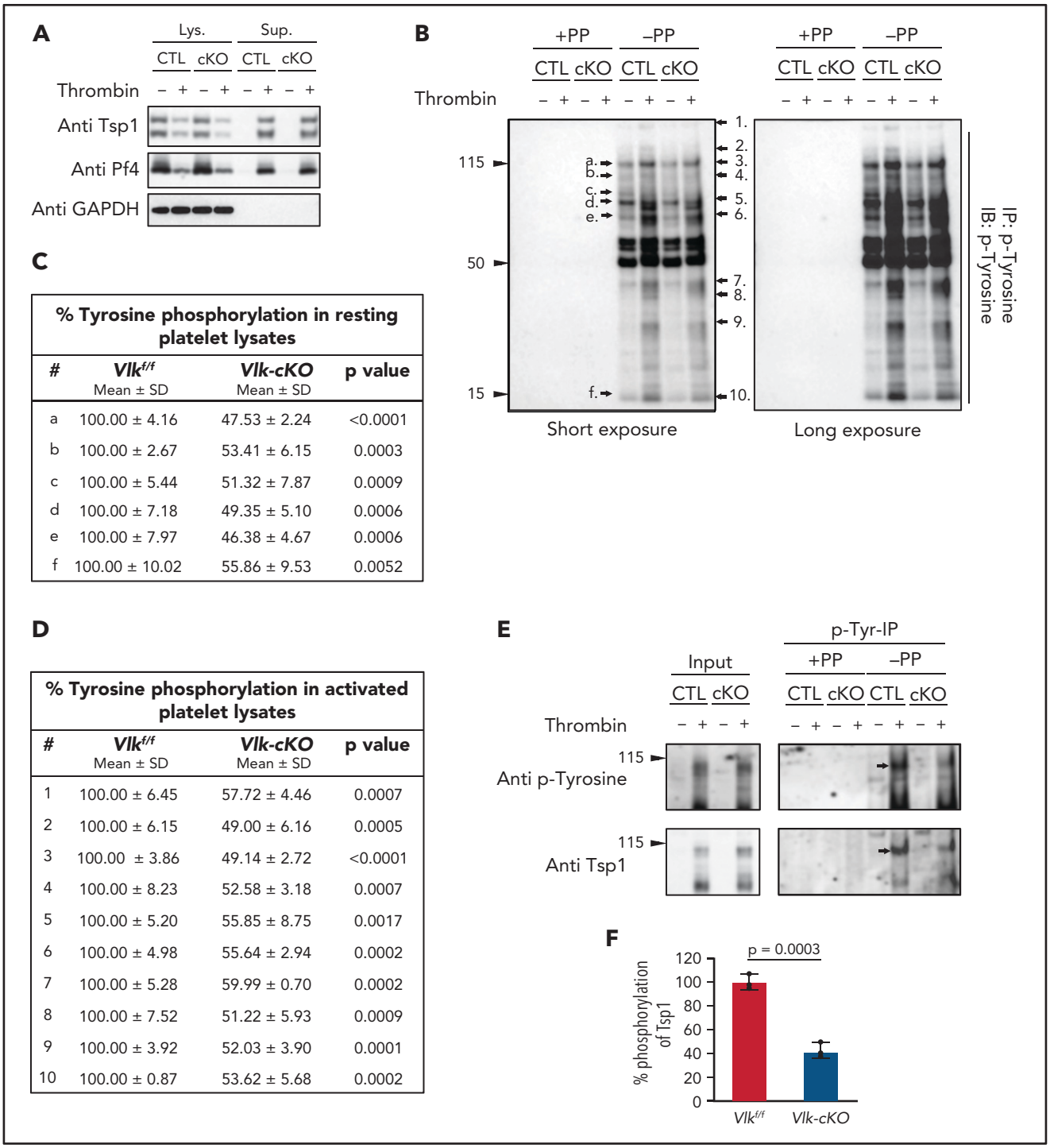

% Tyrosine phosphorylation in resting platelet lysates

#	*Vlk*$^{f/f}$ Mean ± SD	*Vlk-cKO* Mean ± SD	p value
a	100.00 ± 4.16	47.53 ± 2.24	<0.0001
b	100.00 ± 2.67	53.41 ± 6.15	0.0003
c	100.00 ± 5.44	51.32 ± 7.87	0.0009
d	100.00 ± 7.18	49.35 ± 5.10	0.0006
e	100.00 ± 7.97	46.38 ± 4.67	0.0006
f	100.00 ± 10.02	55.86 ± 9.53	0.0052

% Tyrosine phosphorylation in activated platelet lysates

#	*Vlk*$^{f/f}$ Mean ± SD	*Vlk-cKO* Mean ± SD	p value
1	100.00 ± 6.45	57.72 ± 4.46	0.0007
2	100.00 ± 6.15	49.00 ± 6.16	0.0005
3	100.00 ± 3.86	49.14 ± 2.72	<0.0001
4	100.00 ± 8.23	52.58 ± 3.18	0.0007
5	100.00 ± 5.20	55.85 ± 8.75	0.0017
6	100.00 ± 4.98	55.64 ± 2.94	0.0002
7	100.00 ± 5.28	59.99 ± 0.70	0.0002
8	100.00 ± 7.52	51.22 ± 5.93	0.0009
9	100.00 ± 3.92	52.03 ± 3.90	0.0001
10	100.00 ± 0.87	53.62 ± 5.68	0.0002

Figure 3. Reduced tyrosine phosphorylation in resting and activated mouse platelets harboring deletion of *Vlk* compared with control. (A) Immunoblots of lysates (Lys.) and supernatants (Sup.) from *Vlk*$^{f/f}$ (CTL) and *Vlk-cKO* (cKO) platelets resting or stimulated with 5 U/mL thrombin for 15 minutes. Anti-Tsp1 and anti-PF4 antibodies were used as markers of platelet activation, and anti-GAPDH antibody was used to examine total protein levels in lysates. (B) Lysates from panel A were used to examine tyrosine phosphoproteins by immunoblot (IB) of p-Tyr–enriched fraction (IP). Black arrows indicate phosphobands decreased in *Vlk-cKO* (cKO) compared with *Vlk*$^{f/f}$ (CTL) in resting (a-f) and activated (1-10) platelets. Cumulative percent tyrosine phosphorylation in phosphorylated proteins indicated in representative figure in panel B from resting (C) and activated (D) control and *Vlk-cKO* lysates. Data are expressed as mean ± standard deviation (SD); n = 3 independent experiments. Quantifications were normalized to GAPDH protein expression. (E) Representative image of input and p-Tyr IP fraction from resting and thrombin-stimulated supernatants analyzed by using SDS-polyacrylamide gel electrophoresis (PAGE) with 8% gels and immunoblotting with anti–p-Tyr and anti-Tsp1 antibodies. Phenyl phosphate (PP) was used as negative control for nonspecific binding to p-Tyr beads. Black arrows indicate bands decreasing in cKO compared with CTL. (F) Cumulative percent phosphorylation of Tsp1 in activated supernatants from *Vlk-cKO* compared with CTL; n = 3 independent experiments.

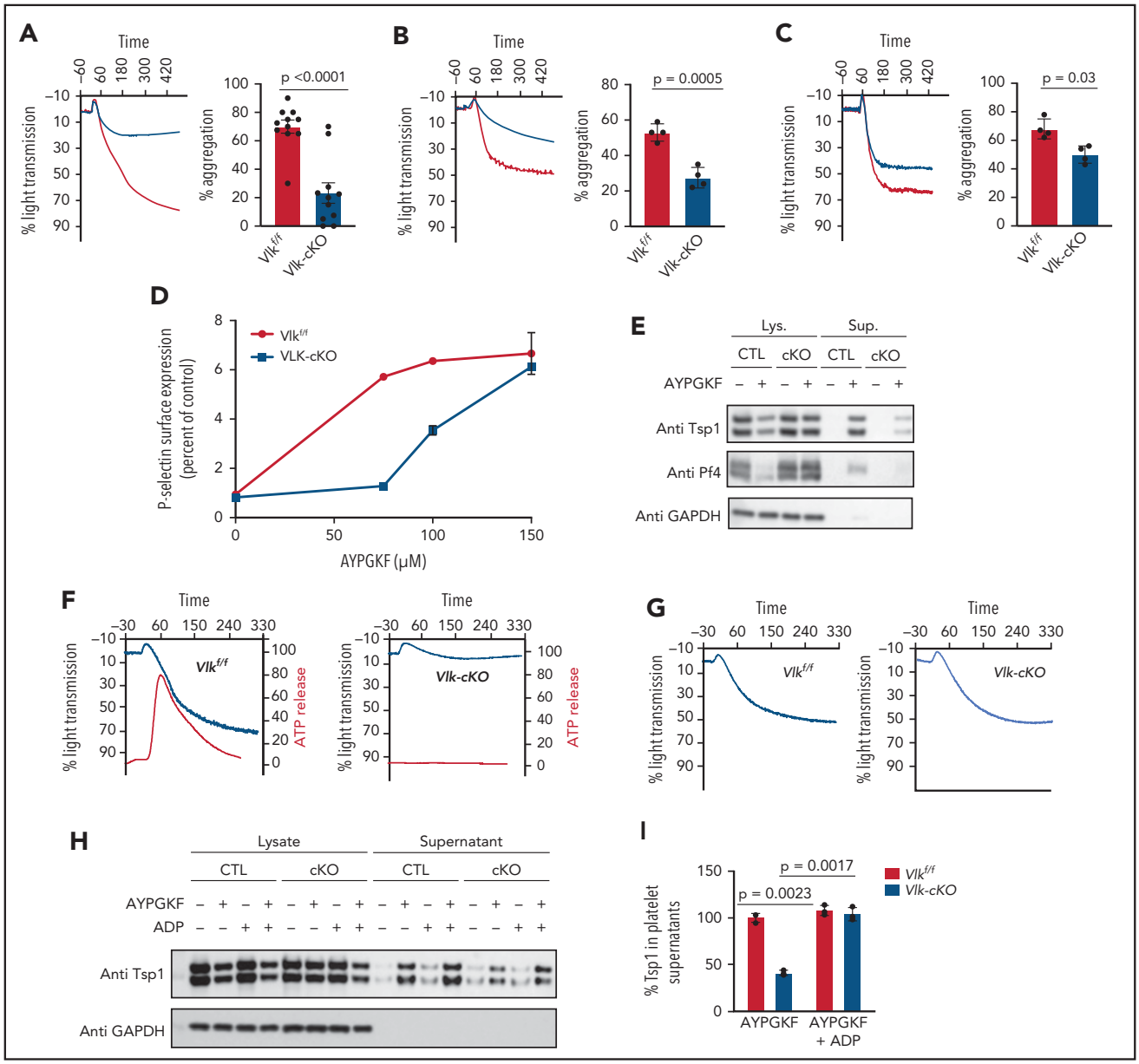

Figure 4. *Vlk* deficiency in platelets alters platelet aggregation and granule exocytosis. Evaluation of aggregation of washed platelets (2×10^8 platelets/mL) from control mice (gray) and platelet-specific VLK knockout mice (blue) stimulated with 100 μM PAR4 peptide AYPGKF (n = 11 per group) (A), 4 mg/mL collagen (n = 4 per group) (B), or 0.4 U/mL thrombin (n = 4 per group) (C). Representative tracings are shown in left panel and cumulative data in right panel. (D) Expression of P-selectin in platelets from control (gray) and platelet-specific VLK knockout mice (blue) in response to AYPGKF. (E) Protein immunoblots of lysates (Lys.) and supernatants (Sup.) from *Vlk*$^{f/f}$ (CTL) and *Vlk-cKO* (cKO) platelets resting or stimulated with 100 μM PAR4 peptide AYPGKF for 15 minutes. Anti-Tsp1 and anti-PF4 antibodies were used to detect secretion of α-granule cargo, and anti-GAPDH antibody was used to determine total protein levels in lysates. (F) Concurrent monitoring of aggregation (blue tracing) and ATP release (red tracing) after exposure to 50 μM AYPGKF in platelets from control (left panel) and platelet-specific VLK knockout mice (right panel). (G) Aggregation studies in platelets from control (left panel) and platelet-specific VLK knockout mice (right panel) were performed as described in panel E except that ADP 2.5 μM was added together with AYPGKF. (H) Representative image of protein immunoblots of lysates and supernatants from CTL and cKO platelets resting or stimulated with 100 μM AYPGKF and/or 2.5 μM ADP for 15 minutes. Anti-Tsp1 antibody was used to detect secretion of α-granule cargo, and anti-GAPDH antibody was used to determine total protein levels. (I) Cumulative percent levels of Tsp1 in supernatants from CTL and cKO platelets stimulated with 100 μM AYPGKF and 2.5 μM ADP; n = 3 independent experiments. Quantifications were normalized to GAPDH protein expression.

Vlk$^{f/f}$; *Pf4-Cre* mice (*Vlk-cKO*). Analysis of genomic DNA from *Vlk-cKO* mice revealed the presence of the targeted loxP and Pf4-Cre alleles (Figure 2A). *Vlk-cKO* mice were born in normal numbers and survived until adulthood. They were normal weight and had no gross morphologic defects. Platelets isolated from these mice exhibited a substantial decrease in VLK, as evaluated by western blot analysis (*Vlk*$^{f/f}$, 100.0 ± 15.7% [n = 2]; *Vlk-cKO*, 4.2 ± 2.0% [n = 2]) (Figure 2B). In contrast, P-selectin and GAPDH levels were indistinguishable between control and VLK knockout platelets, indicating equal protein loading. Complete blood counts were performed to identify any gross abnormalities in hematopoiesis resulting from platelet-specific deficiency of VLK. No significant differences in leukocyte, erythrocyte, or platelet counts were observed between *Vlk-cKO* mice and controls (supplemental Table 3). Similarly, no differences in mean platelet volume were observed. Evaluation of platelets by using

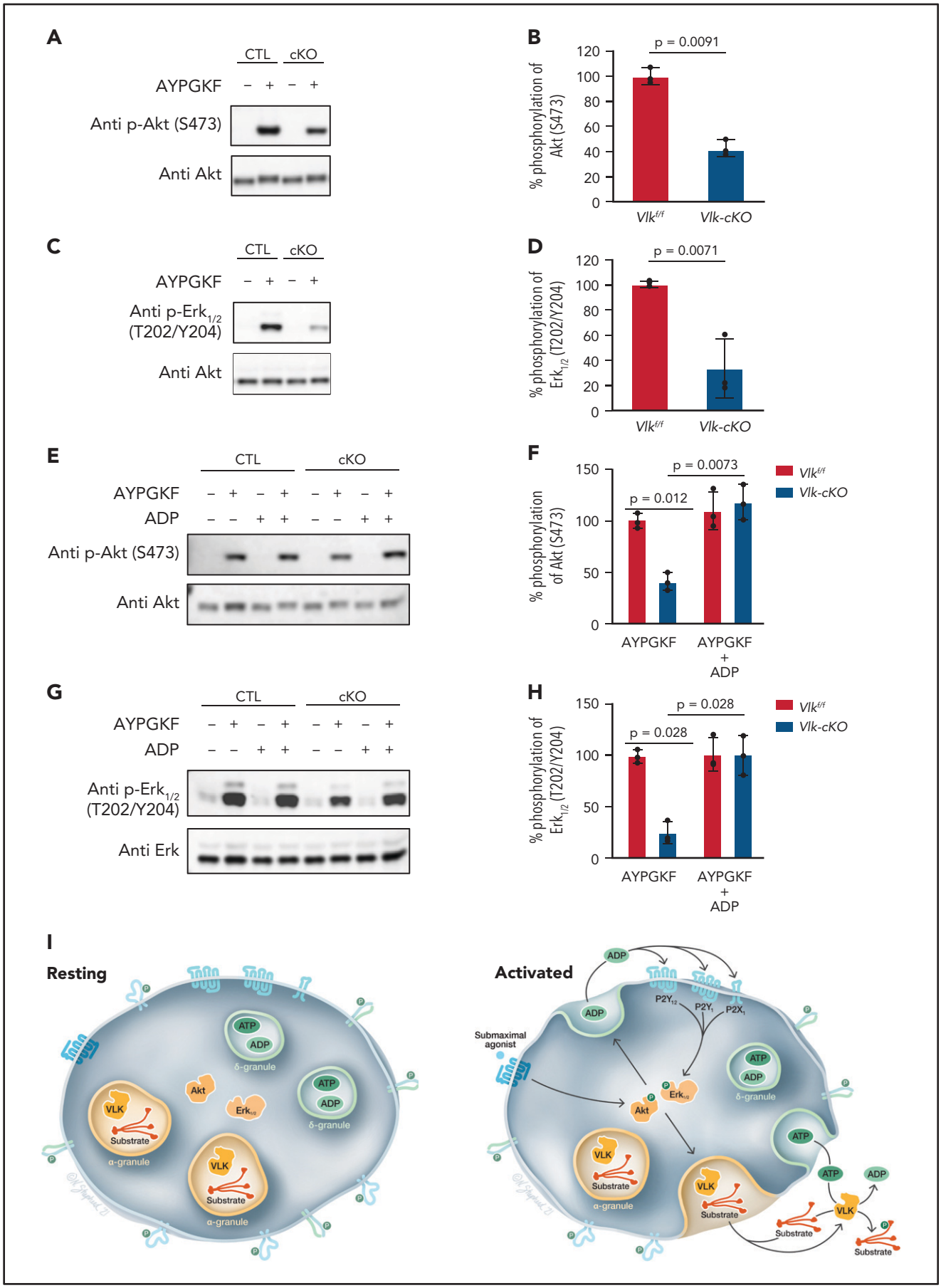

Figure 5. Evaluation of proximal signaling in VLK-deficient platelets. (A) Representative image of p-Akt (S473) and total Akt levels in lysates from CTL and cKO platelets resting or stimulated with 100 μM AYPGKF. (B) Cumulative percent phosphorylation of S473 in Akt; n = 3 independent experiments. (C) Representative image

transmission electron microscopy revealed normal platelet morphology and did not indicate any obvious differences in platelet shape or organelle number (Figure 2C). Dense granules and α-granules in VLK-deficient platelets were intact and were similar in size and morphology to controls. Western blot analysis of lysates from wild-type and VLK-deficient platelets exhibited a normal complement of the major platelet surface receptors $\alpha_{2b}\beta_3$, glycoprotein Ibα, and P-selectin (Figure 2D) and the major secretory proteins fibrinogen, von Willebrand factor, and PF4 (Figure 2E).

To determine whether deficiency of VLK in platelets affects activation-dependent tyrosine phosphorylation, control and VLK-deficient platelets were stimulated with thrombin to elicit full activation. Secretory proteins, including Tsp1 and PF4, were evaluated in the lysates and supernatants to show that VLK deficiency did not alter release of granule contents under these conditions of full activation (Figure 3A). In addition, the presence of VLK was detected in the supernatant of thrombin-stimulated human and mouse platelets (supplemental Figure 1A-B). Phosphoproteins phosphorylated at tyrosine residues were then immunoprecipitated from lysates of control and VLK-deficient platelets before and after thrombin stimulation. Western blot analysis revealed several proteins that were tyrosine phosphorylated in resting platelets (Figure 3B, *a-f*) and following platelet activation (Figure 3B, *1-10*). Specificity of the immunoprecipitation was shown by inhibition using phenyl phosphate. Comparison of band intensities from several representative bands obtained from western blots of resting platelets showed decreased phosphorylation of numerous proteins in VLK-deficient platelets relative to controls (Figure 3C). Analysis of tyrosine phosphorylation of activated platelets also showed decreased phosphorylation in VLK-deficient platelets compared with controls (Figure 3D). The secreted protein Tsp1 has been previously identified as a tyrosine phosphorylated protein in platelets (supplemental Table 1). A significant decrease in tyrosine phosphorylation of Tsp1 was observed in VLK-deficient platelets compared with controls (Figure 3E-F; supplemental Figure 1C). These studies show that VLK is secreted from thrombin-activated mouse platelets, and tyrosine phosphorylation is decreased in platelets deficient in VLK. The changes in tyrosine phosphorylation in *VLK-cKO* platelets include secreted proteins such as Tsp1.

Role of VLK in platelet function

To evaluate the effect of VLK deficiency on platelet function, we first compared aggregation of VLK-deficient platelets vs control platelets using a variety of agonists. Although VLK-deficient platelets exhibited complete aggregation in response to full-dose (5 U/mL) thrombin (supplemental Figure 2), defects in platelet function were observed with submaximal doses of agonists. VLK-deficient platelets showed reduced aggregation in response to stimulation of protease-activated receptor 4 (PAR4) with 100 μM AYPGKF compared with $Vlk^{f/f}$ controls ($Vlk^{f/f}$, 70 ± 5.1% aggregation [n = 10]; *Vlk-cKO*, 23 ± 8.0% aggregation [n = 10]) (Figure 4A). Aggregation in response to stimulation with 4 μg/mL collagen was also reduced in VLK-deficient platelets ($Vlk^{f/f}$, 53 ± 2.5% aggregation [n = 4]; *Vlk-cKO*, 27.5 ± 2.9% aggregation [n = 4]) (Figure 4B). There was also a small decrease in aggregation in response to 0.4 U/mL thrombin ($Vlk^{f/f}$, 68 ± 2.3% aggregation [n = 4]; *Vlk-cKO*, 50 ± 2.0% aggregation [n = 4]) (Figure 4C). A dose curve of platelet α-granule release as detected by PAR4-mediated appearance of P-selectin at the surface showed impaired responses at 100 μM AYPGKF but was overcome at 150 μM AYPGKF (Figure 4D). Release of α-granule cargo was also decreased in *Vlk-cKO* platelets, as evidenced by reduction of Tsp1 and PF4 secretion in response to 100 μM AYPGKF (Figure 4E). Dense granule release in control platelets occurred in response to 50 μM AYPGKF but was absent in platelets that lack VLK (Figure 4F). Addition of a subthreshold concentration of adenosine 5′-diphosphate (ADP) (2.5 μM) restored platelet aggregation in *Vlk-cKO* platelets (Figure 4G). Furthermore, platelet aggregation in response to ADP was comparable between control and *Vlk-cKO* platelets, regardless of the dose that was used (supplemental Figure 3). ADP supplementation also restored release of α-granule cargo in *Vlk-cKO* platelets, as evidenced by comparable levels of Tsp1 secretion by $Vlk^{f/f}$ and *Vlk-cKO* platelets in response to 100 μM AYPGKF and 2.5 μM ADP (Figure 4H-I). These studies indicate that deficiency of VLK impairs platelet function in response to low to moderate doses of agonists other than ADP.

To further evaluate the platelet function defect in the absence of VLK, proximal signaling events in response to agonist stimulation were monitored. Exposure of platelets to 100 μM AYPGKF resulted in phosphorylation of Akt (S473) and $Erk_{1/2}$ (T202/Y204). Specifically, Akt (S473) phosphorylation was reduced by 63 ± 18.6% in *Vlk-cKO* compared with control platelets (Figure 5A-B). $Erk_{1/2}$ (T202/Y204) phosphorylation was also reduced by 67.6 ± 21.9% in *Vlk-cKO* compared with controls (Figure 5C-D). Similar to the observations made for platelet aggregation and α-granule cargo release, phosphorylation of Akt (S473) and $Erk_{1/2}$ (T202/Y204) was restored in *Vlk-cKO* platelets in response to 100 μM AYPGKF and 2.5 μM ADP (Figure 5E-H). Taken together, our analysis of platelet function in *Vlk-cKO* platelets indicates that VLK influences release of platelet-dense granules and that its absence results in platelets that are less sensitive to platelet activation but capable of full activation in response to strong agonists (Figure 5I).

Figure 5 (continued) of p-$Erk_{1/2}$ (T202/Y204) and $Erk_{1/2}$ total levels in lysates from CTL and cKO platelets resting or stimulated with 100 μM AYPGKF. (D) Cumulative percent phosphorylation of $Erk_{1/2}$; n = 3 independent experiments. (E) Representative image of p-Akt (S473) and total Akt levels in lysates from CTL and cKO platelets resting or stimulated with 100 μM AYPGKF and/or 2.5 μM ADP. (F) Cumulative percent phosphorylation of S473 in Akt; n = 3 independent experiments. (G) Representative image of p-$Erk_{1/2}$ (T202/Y204) and $Erk_{1/2}$ total levels in lysates from CTL and cKO platelets resting or stimulated with 100 μM AYPGKF and/or 2.5 μM ADP. (H) Cumulative percent phosphorylation of $Erk_{1/2}$; n = 3 independent experiments. (I) Proposed model for the role of VLK in platelet function. Resting platelet: Proteins that are tyrosine phosphorylated by VLK in the megakaryocyte secretory pathway during thrombopoiesis are present in extracellular domains of surface proteins or intragranular proteins of resting platelets. VLK is localized to α-granules. ADP and ATP are concentrated in dense granules. Activated platelet: Activation with a submaximal agonist results in partial activation of kinases involved in dense granule release, such as Akt and $Erk_{1/2}$. Signaling downstream of Akt and $Erk_{1/2}$ results in release of ADP from dense granules. VLK appears to act in these steps leading to dense granule release by mechanisms that are yet to be determined but could include phosphorylation of receptors on extracellular domains, phosphorylation of secretory chaperones, or phosphorylation of dense granule resident proteins important for release. ADP released from dense granules stimulates purinergic receptors, enhancing signaling through kinases involved in granule release. Agonist stimulation also causes exocytosis of α-granules, resulting in the release of VLK into the extracellular environment along with ATP and VLK substrates.

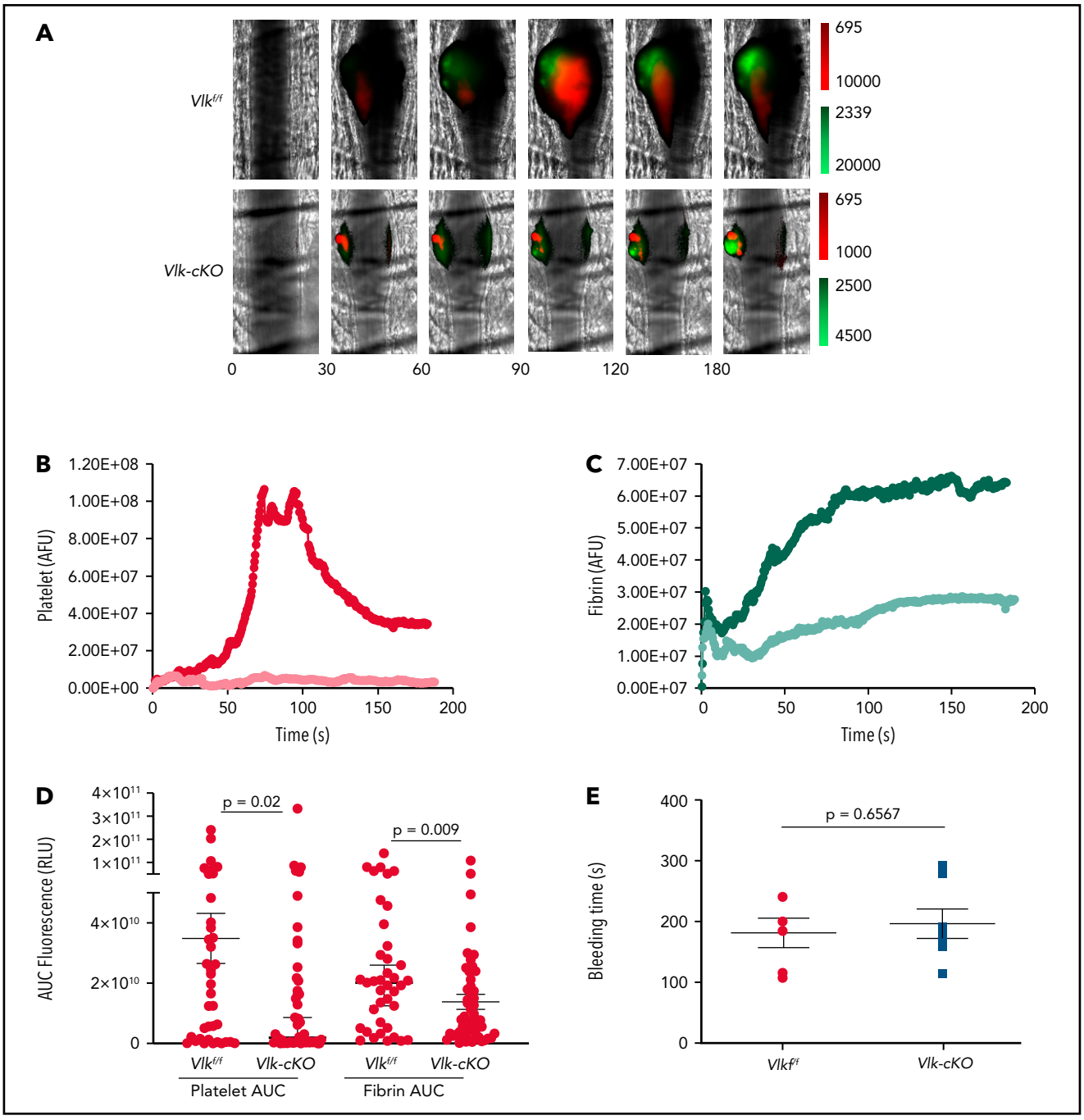

Figure 6. Ablation of *Vlk* in platelet lineage reduces arterial thrombosis without affecting bleeding times. (A-D) Cremaster arteriole injury was induced by laser ablation in *Vlk-cKO* mice and *Vlk*$^{f/f}$ littermate control mice. Platelet and fibrin accumulation at the site of injury was detected for 180 seconds with DyLight 647–labeled platelet-specific anti-CD42b antibody (0.1 μg/g body weight) and DyLight 488–labeled anti-fibrin antibody (59D8, 0.5 μg/g body weight), respectively. (A) Representative images from a single thrombus evaluated for the appearance of fluorescence signals associated with platelet accumulation (red) and fibrin deposition (green) at indicated time points postinjury (lookup tables at right of images). Median integrated platelet (red) (B) and fibrin (green) (C) fluorescent intensities after laser-induced injury were calculated for all thrombi in *Vlk*$^{f/f}$ (n = 3; 39 thrombi, darker color) and *Vlk-cKO* (n = 3; 52 thrombi, lighter color) mice. (D) Area under the curve (AUC) for platelet and fibrin fluorescent intensities was calculated for all individual thrombi. Error bars represent the median with 95% confidence intervals. (E) Time to bleeding cessation (seconds) in *Vlk*$^{f/f}$ (n = 6), and *Vlk-cKO* (n = 7) mice (unpaired Student *t* test, $P = .6567$).

Platelet VLK functions in thrombus formation in vivo

The observation that platelet VLK functions in aggregation and granule release in response to submaximal concentrations of agonists raises the question of whether it is important in thrombus formation. To address this possibility, we evaluated platelet accumulation and fibrin formation after laser-induced injury of cremaster arterioles using intravital microscopy. Platelet accumulation in *Vlk-cKO* mice was reduced to 90% of that of control mice ($P \leq .02$) (Figure 6A-B,D). In addition, fibrin formation in *Vlk-cKO* mice was reduced to 62% of that of control mice ($P \leq .009$) (Figure 6A,C,D).

We next evaluated the effect of megakaryocyte/platelet-specific VLK deficiency on tail bleeding times. In contrast to their defective thrombus formation after arteriolar injury, *Vlk-cKO* mice did not exhibit prolonged tail bleeding times (Figure 6E). Thus, for the assays used in this study, *Vlk-cKO* mice showed a defect in thrombus formation but not bleeding.

Discussion

Although numerous instances of protein kinase localization and activity in the platelet extracellular environment have been described over the years,[33-36] the reported kinases (ie, PKA, PKC) are cytoplasmic kinases with no known mechanism for regulated release, and their extracellular localization may be secondary to nonspecific cell breakage. Because there have been no genetic approaches to test the role of these putative extracellular activities, their functional significance has remained obscure. We report here the first functional data on a protein kinase that is specifically localized to the secretory pathway in platelets, VLK. We describe a role for platelet VLK in aggregation, granule exocytosis, and thrombus formation. Depletion of VLK did not affect platelet count or volume, nor did it cause any gross abnormalities in platelet morphology or changes in blood cell indices (Figure 2; supplemental Table 3). Immunofluorescence confocal imaging and transmission electron microscopy have shown that platelet VLK is sequestered in platelet α-granules.[7] This localization is consistent with the presence of a N-terminal hydrophobic sequence in VLK that targets it to the secretory pathway. How VLK might be enriched in α-granules will be an interesting area for future investigation. Platelets lacking VLK show no defect in α-granule morphology, number, or secretory pathway protein content, suggesting that VLK is not necessary for normal α-granule biogenesis.

Several lines of evidence point to a dose-sensitive defect in stimulus-dependent dense granule release in VLK-deficient platelets. Platelets exhibited impaired aggregation in response to activation by a PAR4 agonist, collagen, and low-dose thrombin but not in response to ADP (Figure 4; supplemental Figure 3). ADP release from dense granules contributes to stimulation of platelets with submaximal agonist concentrations[37-42] but is not important for platelet aggregation in response to exogenously added ADP. Tracings from VLK-deficient platelets showed a lack of dense granule release in response to submaximal concentrations of the PAR4 agonist AYPGKF (Figure 4E), and addition of a subthreshold amount of ADP completely reversed the aggregation defect (Figure 4F). Taken together, these observations strongly indicate that dense granule release is impaired in VLK-deficient platelets. A primary defect in dense granule release could also impair α-granule exocytosis.[41] However, it is not clear that the defect in dense granule release is due to an intrinsic dense granule defect or a defect in upstream signaling that is required for granule release. The facts that the initial wave of platelet aggregation (before dense granule release) (Figure 4E) and that Akt (Figure 5A-B) and $Erk_{1/2}$ (Figure 5C-D) phosphorylation are inhibited in VLK-deficient platelets suggest that the primary defect is upstream of dense granule release.

Our in vivo studies establish that thrombus formation is impaired in *Vlk-cKO* mice after arteriolar injury (Figure 6), consistent with the defects in platelet exocytosis and aggregation we find in purified platelets. Other genetically modified mice with impaired platelet granule release have also shown significant defects in thrombus formation.[39,43,44] Thus, the defect in accumulation of VLK-deficient platelets after vascular injury may be due to a primary secretion defect, impaired extracellular tyrosine phosphorylation, or both. It is possible that the observed decrease in fibrin formation (Figure 6A,C-D) is secondary to the defect in platelet accumulation (Figure 6A-B,D), resulting in a decreased surface for fibrin formation. Previous studies using the laser-induced injury model in PAR4-deficient mice have shown, however, that impairment of platelet accumulation does not prevent fibrin formation,[45,46] suggesting that a platelet aggregation defect may not be sufficient to account for defects in fibrin formation associated with VLK loss. Data pointing to the endothelial monolayer as the primary surface for fibrin formation after laser-induced injury also suggest that the fibrin and platelet aggregation defects result from distinct effects of VLK loss.[46,47] Interestingly, fibrinogen has been reported to be tyrosine phosphorylated in vivo (supplemental Table 1),[17] raising the possibility of a more direct effect of VLK on fibrin formation. Defective thrombus formation in the absence of prolongation of bleeding times, as observed in mice with platelet-specific loss of VLK, raises the possibility of inhibiting clotting without increasing the risk of hemorrhage, but this theory requires explanation. Thrombus formation is more sensitive to defects in granule secretion than is hemostasis. Joshi et al[48] showed that a ~40% to 50% reduction in platelet secretion in vitro correlated with reduced thrombus formation but no compromise in hemostasis as measured by tail clip assay. Differences in the role of fluid dynamics, vessel contraction, relative contribution of the coagulation cascade, and other factors may account for this apparent discrepancy.

Previous work has established that VLK can phosphorylate secreted proteins both in the secretory pathway and after its release from α-granules.[7] We now show that Tsp1 is a VLK substrate in platelets (Figure 3E-F; supplemental Figure 1C). The role of VLK in extracellular phosphorylation after release is particularly intriguing in platelets, because adenosine triphosphate (ATP) is released from dense granules concomitant with release of VLK and substrates from α-granules (Figure 5I). We have observed reduced phosphorylation of extracellular tyrosine phosphorylation in Hermansky-Pudlak syndrome platelets, which are deficient in ADP/ATP, suggesting that release of ATP from dense granules is indeed critical for VLK activity in the extracellular environment (supplemental Figure 4). Our findings that VLK-deficient platelets are defective in dense granule release (Figures 4F-I and 5E-H), however, indicate that a key functional defect in these platelets is before the stimulus-dependent release of ATP, either in the early steps in receptor activation or in stimulus-dependent dense granule mobilization. It therefore seems likely that VLK is required in the secretory pathway, either during platelet development or in the resting mature platelet, for normal coupling of agonist stimulation to dense granule release. Although VLK depletion results in impaired agonist-stimulated dense granule release (Figure 4F), ADP-mediated activation of purinergic receptors remains unaffected (supplemental Figure 3), indicating that this defect is not due to a generalized defect in platelet activation. Phosphorylation of receptors on extracellular domains, secretory chaperones necessary for receptor surface expression, and dense granule resident proteins important for release are each a possibility for how VLK might be required for normal stimulus-response coupling in platelets. In any

case, kinase activity of VLK after stimulus-dependent cosecretion with ATP is unlikely to explain this phenotype. Tyrosine phosphorylation of the extracellular domain of ENTPD6 in the absence, as well as presence, of platelet activation (Figure 1) likewise suggests that tyrosine phosphorylation in the secretory pathway before platelet activation may be important in the regulation of platelet responsiveness.

There may be, however, an important role for postrelease activity of platelet VLK in thrombus formation in vivo. Tyrosine phosphorylation of a broad range of secreted proteins implicated in thrombosis, angiogenesis, and wound healing has been identified in human and mouse tissue samples,[49] and we have found many of these same phosphorylations both in human platelets (Figure 1B) or after expression of VLK in cultured cells.[7] Platelets are not the only potential source of VLK in the thrombosis/wound microenvironment, as VLK is present at significant levels in circulating plasma,[50] and sorting out the full complexity of VLK sources and targets under in vivo circumstances will be a long-term undertaking. Although mice lacking VLK in specific tissues are an essential tool for defining the function of VLK in hemostasis and wound healing, the very small amounts of material available from wound sites in mice are not sufficient for the identification of tyrosine-phosphorylated secreted proteins by liquid chromatography/tandem mass spectrometry analysis. This limitation currently precludes us from directly identifying candidate VLK target phosphoproteins from sites of local arteriole damage. Further study of tyrosine phosphoproteins and VLK-dependent phosphorylations in alternate systems (eg, tissue culture, large animal thromboses) are likely to identify candidate targets that can be interrogated in the murine system.

We have shown that megakaryocyte/platelet-specific deletion of VLK results in platelet function defects and reduced thrombus formation. These observations, particularly the finding that deletion of VLK inhibits thrombus formation without prolonging bleeding times, raise the possibility that pharmacologic inhibition of VLK could represent a novel therapeutic strategy in thrombosis. VLK is widely divergent from cytoplasmic kinases, has extra-cytoplasmic localization, and postnatal deletion of VLK is well tolerated (unpublished data generated by David Maridas and L.R. including animal viability, length, weight, micro-computed tomography of the long bones, and organ morphology from various tissues such as liver, lung, heart and brain), allowing VLK to be targeted distinctively from the rest of the kinome. Detailed phenotyping of resting VLK-deficient platelets showed that the only detectable defect resulting from VLK deficiency is altered tyrosine phosphorylation. Overall, these results show that VLK is essential for normal platelet function and thrombus formation, and implicate tyrosine phosphorylation of extracellular protein functions in thrombosis.

Acknowledgments

The authors thank Nicole Shepherd for creating the illustration in Figure 5I and Kristen Powers for her assistance generating the human ENTPD6-V5 plasmid.

M.W. has received support from the National Institutes of Health, National Institute of General Medical Sciences (R01GM115417), the National Institute of Arthritis and Musculoskeletal and Skin Diseases (R01AR066717), and the National Institute of Dental and Craniofacial Research (R21DE024312). R.F. has received support from the National Heart, Lung, and Blood Institute (R35HL135775 and R01HL125275). J.E.I. has received support from the National Heart, Lung, and Blood Institute (R01HL068130 and R01HL136394).

Authorship

Contribution: L.R. designed, performed, and analyzed experiments as well as wrote and edited the manuscript; G.M.-S., K.D.C., J.R.D., M.R.B., C.G.P., A.I., S.G., and L.N. performed experiments and analyzed data; J.E.I. and V.R. designed experiments and edited the manuscript; and M.W. and R.F. designed and analyzed experiments, and wrote and edited the manuscript.

Conflict-of-interest disclosure: J.E.I. has financial interests in and is a founder of Platelet BioGenesis, a company that aims to produce donor-independent human platelets from human-induced pluripotent stem cells at scale; he is an inventor on this patent. The interests of J.E.I. were reviewed and are managed by the Brigham and Women's Hospital and Partners HealthCare in accordance with their conflict-of-interest policies. R.F. has financial interests in and is a founder of PlateletDiagnostics. His interests are reviewed and managed by Beth Israel Deaconess Medical Center in accordance with their conflict-of-interest policies. The remaining authors declare no competing financial interests.

ORCID profile: S.G., 0000-0002-0542-1221.

Correspondence: Malcolm Whitman, Department of Developmental Biology, Harvard School of Dental Medicine, 188 Longwood Ave, Boston, MA 02115; e-mail: Malcolm_Whitman@hms.harvard.edu; and Robert Flaumenhaft, Division of Hemostasis and Thrombosis, Department of Medicine, Beth Israel Deaconess Medical Center, 330 Brookline Ave, Boston, MA 02215; e-mail: rflaumen@bidmc.harvard.edu.

Footnotes

Submitted 9 December 2020; accepted 22 July 2021; prepublished online on *Blood* First Edition 30 July 30, 2021. DOI 10.1182/blood.2020010342.

*M.W. and R.F. contributed equally to the manuscript.

Requests for original data may be submitted to malcolm_whitman@hms.harvard.edu or rflaumen@bidmc.harvard.edu.

The online version of this article contains a data supplement.

There is a *Blood Commentary* on this article in this issue.

The publication costs of this article were defrayed in part by page charge payment. Therefore, and solely to indicate this fact, this article is hereby marked "advertisement" in accordance with 18 USC section 1734.

REFERENCES

1. Hammersten O. Zur Frage, ob das Casein ein einheitlicher Stoff sei. *Hoppe Seylers Z Physiol Chem*. 1883;7:227-273.
2. Tagliabracci VS, Pinna LA, Dixon JE. Secreted protein kinases. *Trends Biochem Sci*. 2013;38(3):121-130.
3. Tagliabracci VS, Engel JL, Wen J, et al. Secreted kinase phosphorylates extracellular proteins that regulate biomineralization. *Science*. 2012;336(6085):1150-1153.
4. Ishikawa HO, Takeuchi H, Haltiwanger RS, Irvine KD. Four-jointed is a Golgi kinase that phosphorylates a subset of cadherin domains. *Science*. 2008;321(5887):401-404.
5. Wen J, Xiao J, Rahdar M, et al. Xylose phosphorylation functions as a molecular switch to regulate proteoglycan biosynthesis. *Proc Natl Acad Sci USA*. 2014;111(44):15723-15728.

6. Yoshida-Moriguchi T, Willer T, Anderson ME, et al. SGK196 is a glycosylation-specific O-mannose kinase required for dystroglycan function. *Science*. 2013;341(6148):896-899.

7. Bordoli MR, Yum J, Breitkopf SB, et al. A secreted tyrosine kinase acts in the extracellular environment [published correction appears in *Cell*. 2014;159(4):955]. *Cell*. 2014;158(5):1033-1044.

8. Kinoshita M, Era T, Jakt LM, Nishikawa S. The novel protein kinase Vlk is essential for stromal function of mesenchymal cells. *Development*. 2009;136(12):2069-2079.

9. Harada H, Farhani N, Wang X-F, et al. Extracellular phosphorylation drives the formation of neuronal circuitry. *Nat Chem Biol*. 2019;15(11):1035-1042.

10. Kim JM, Han H, Bahn M, Hur Y, Yeo CY, Kim DW. Secreted tyrosine kinase Vlk negatively regulates Hedgehog signaling by inducing lysosomal degradation of Smoothened. *Biochem J*. 2020;477(1):121-136.

11. Maddala R, Skiba NP, Rao PV. Vertebrate lonesome kinase regulated extracellular matrix protein phosphorylation, cell shape, and adhesion in trabecular meshwork cells. *J Cell Physiol*. 2017;232(9):2447-2460.

12. Farhan H. Tyrosine kinase signaling in and on the endoplasmic reticulum. *Biochem Soc Trans*. 2020;48(1):199-205.

13. Imuta Y, Nishioka N, Kiyonari H, Sasaki H. Short limbs, cleft palate, and delayed formation of flat proliferative chondrocytes in mice with targeted disruption of a putative protein kinase gene, Pkdcc (AW548124). *Dev Dyn*. 2009;238(1):210-222.

14. Estrada K, Styrkarsdottir U, Evangelou E, et al. Genome-wide meta-analysis identifies 56 bone mineral density loci and reveals 14 loci associated with risk of fracture. *Nat Genet*. 2012;44(5):491-501.

15. Machado JP, Johnson WE, Gilbert MTP, et al. Bone-associated gene evolution and the origin of flight in birds. *BMC Genomics*. 2016;17(1):371.

16. Sajan SA, Ganesh J, Shinde DN, et al. Biallelic disruption of *PKDCC* is associated with a skeletal disorder characterised by rhizomelic shortening of extremities and dysmorphic features. *J Med Genet*. 2019;56(12):850-854.

17. Izquierdo I, Barrachina MN, Hermida-Nogueira L, et al. A Comprehensive tyrosine phosphoproteomic analysis reveals novel components of the platelet CLEC-2 signaling cascade. *Thromb Haemost*. 2020;120(2):262-276.

18. Beck F, Geiger J, Gambaryan S, et al. Temporal quantitative phosphoproteomics of ADP stimulation reveals novel central nodes in platelet activation and inhibition. *Blood*. 2017;129(2):e1-e12.

19. Zahedi RP, Lewandrowski U, Wiesner J, et al. Phosphoproteome of resting human platelets. *J Proteome Res*. 2008;7(2):526-534.

20. Maguire PB, Wynne KJ, Harney DF, O'Donoghue NM, Stephens G, Fitzgerald DJ. Identification of the phosphotyrosine proteome from thrombin activated platelets. *Proteomics*. 2002;2(6):642-648.

21. Breitkopf SB, Asara JM. Determining in vivo phosphorylation sites using mass spectrometry. *Curr Protoc Mol Biol*. 2012;Chapter18:Unit18.19.1-27.

22. Probst S, Zeller R, Zuniga A. The hedgehog target Vlk genetically interacts with Gli3 to regulate chondrocyte differentiation during mouse long bone development. *Differentiation*. 2013;85(4-5):121-130.

23. Tiedt R, Schomber T, Hao-Shen H, Skoda RC. Pf4-Cre transgenic mice allow the generation of lineage-restricted gene knockouts for studying megakaryocyte and platelet function in vivo. *Blood*. 2007;109(4):1503-1506.

24. Truett GE, Heeger P, Mynatt RL, et al. Preparation of PCR-quality mouse genomic DNA with hot sodium hydroxide and tris (HotSHOT). *Biotechniques*. 2000;29(1):52-54.

25. De Ceunynck K, Peters CG, Jain A, et al. PAR1 agonists stimulate APC-like endothelial cytoprotection and confer resistance to thromboinflammatory injury. *Proc Natl Acad Sci USA*. 2018;115(5):E982-E991.

26. Jasuja R, Passam FH, Kennedy DR, et al. Protein disulfide isomerase inhibitors constitute a new class of antithrombotic agents. *J Clin Invest*. 2012;122(6):2104-2113.

27. Bekendam RH, Iyu D, Passam F, et al. Protein disulfide isomerase regulation by nitric oxide maintains vascular quiescence and controls thrombus formation. *J Thromb Haemost*. 2018;16(11):2322-2335.

28. Matsuura S, Thompson CR, Belghasem ME, et al. Platelet dysfunction and thrombosis in $JAK2^{V617F}$-mutated primary myelofibrotic mice. *Arterioscler Thromb Vasc Biol*. 2020;40(10):e262-e272.

29. Liu Y, Jennings NL, Dart AM, Du X-J. Standardizing a simpler, more sensitive and accurate tail bleeding assay in mice. *World J Exp Med*. 2012;2(2):30-36.

30. Glenney JRJ Jr, Zokas L, Kamps MP. Monoclonal antibodies to phosphotyrosine. *J Immunol Methods*. 1988;109(2):277-285.

31. Yeung G, Mulero JJ, McGowan DW, Bajwa SS, Ford JE. CD39L2, a gene encoding a human nucleoside diphosphatase, predominantly expressed in the heart. *Biochemistry*. 2000;39(42):12916-12923.

32. Atkinson B, Dwyer K, Enjyoji K, Robson SC. Ecto-nucleotidases of the CD39/NTPDase family modulate platelet activation and thrombus formation: potential as therapeutic targets. *Blood Cells Mol Dis*. 2006;36(2):217-222.

33. Korc-Grodzicki B, Tauber-Finkelstein M, Chain D, Shaltiel S. Vitronectin is phosphorylated by a cAMP-dependent protein kinase released by activation of human platelets with thrombin. *Biochem Biophys Res Commun*. 1988;157(3):1131-1138.

34. Hillen TJ, Aroor AR, Shukla SD. Selective secretion of protein kinase C isozymes by thrombin-stimulated human platelets. *Biochem Biophys Res Commun*. 2001;280(1):259-264.

35. Stavenuiter F, Gale AJ, Heeb MJ. Phosphorylation of protein S by platelet kinases enhances its activated protein C cofactor activity. *FASEB J*. 2013;27(7):2918-2925.

36. Ekdahl KN, Elgue G, Nilsson B. Phosphorylation of coagulation factor XI by a casein kinase released by activated human platelets increases its susceptibility to activation by factor XIIa and thrombin. *Thromb Haemost*. 1999;82(4):1283-1288.

37. Colman RW, Figures WR, Scearce LM, Strimpler AM, Zhou FX, Rao AK. Inhibition of collagen-induced platelet activation by 5′-p-fluorosulfonylbenzoyl adenosine: evidence for an adenosine diphosphate requirement and synergistic influence of prostaglandin endoperoxides. *Blood*. 1986;68(2):565-570.

38. Ryningen A, Jensen BO, Holmsen H. Role of autocrine stimulation on the effects of cyclic AMP on protein and lipid phosphorylation in collagen-activated and thrombin-activated platelets. *Eur J Biochem*. 1999;260(1):87-96.

39. Graham GJ, Ren Q, Dilks JR, Blair P, Whiteheart SW, Flaumenhaft R. Endobrevin/VAMP-8-dependent dense granule release mediates thrombus formation in vivo. *Blood*. 2009;114(5):1083-1090.

40. Koseoglu S, Peters CG, Fitch-Tewfik JL, et al. VAMP-7 links granule exocytosis to actin reorganization during platelet activation. *Blood*. 2015;126(5):651-660.

41. Harper MT, van den Bosch MT, Hers I, Poole AW. Platelet dense granule secretion defects may obscure α-granule secretion mechanisms: evidence from Munc13-4-deficient platelets. *Blood*. 2015;125(19):3034-3036.

42. Elaïb Z, Adam F, Berrou E, et al. Full activation of mouse platelets requires ADP secretion regulated by SERCA3 ATPase-dependent calcium stores. *Blood*. 2016;128(8):1129-1138.

43. Konopatskaya O, Gilio K, Harper MT, et al. PKCalpha regulates platelet granule secretion and thrombus formation in mice. *J Clin Invest*. 2009;119(2):399-407.

44. Meng R, Wu J, Harper DC, et al. Defective release of α granule and lysosome contents from platelets in mouse Hermansky-Pudlak syndrome models. *Blood*. 2015;125(10):1623-1632.

45. Vandendries ER, Hamilton JR, Coughlin SR, Furie B, Furie BC. Par4 is required for platelet thrombus propagation but not fibrin generation in a mouse model of thrombosis. *Proc Natl Acad Sci USA*. 2007;104(1):288-292.

46. Ivanciu L, Krishnaswamy S, Camire RM. New insights into the spatiotemporal localization

of prothrombinase in vivo. *Blood*. 2014; 124(11):1705-1714.

47. Higgins SJ, De Ceunynck K, Kellum JA, et al. Tie2 protects the vasculature against thrombus formation in systemic inflammation. *J Clin Invest*. 2018;128(4):1471-1484.

48. Joshi S, Banerjee M, Zhang J, et al. Alterations in platelet secretion differentially affect thrombosis and hemostasis. *Blood Adv*. 2018;2(17):2187-2198.

49. Hornbeck PV, Kornhauser JM, Tkachev S, et al. PhosphoSitePlus: a comprehensive resource for investigating the structure and function of experimentally determined post-translational modifications in man and mouse. *Nucleic Acids Res*. 2012; 40(database issue):D261-D270.

50. Qian W-J, Monroe ME, Liu T, et al. Inflammation and the Host Response to Injury Large Scale Collaborative Research Program. Quantitative proteome analysis of human plasma following in vivo lipopolysaccharide administration using 16O/18O labeling and the accurate mass and time tag approach. *Mol Cell Proteomics*. 2005;4(5):700-709.